



# Effect of edge preparation technologies on cutting edge properties and tool performance

Wanting Wang<sup>1</sup> · Md Khalid Saifullah<sup>1</sup> · Robert Aßmuth<sup>2</sup> · Dirk Biermann<sup>2</sup> · A. F. M. Arif<sup>1</sup>  · S. C. Veldhuis<sup>1</sup>

Received: 14 August 2019 / Accepted: 11 November 2019 / Published online: 12 December 2019  
© Springer-Verlag London Ltd., part of Springer Nature 2019

## Abstract

Edge preparation has gained widespread use due to its low cost and high impact. Various edge preparation methods are reported in the literature. Choice of edge preparation techniques influences the edge properties and the ensuing tool performance. The current work investigates the influence of three different edge preparation methods, brushing, drag finishing, and wet abrasive jet machining on the performance of tungsten carbide inserts during orthogonal turning. Edge preparation not only changes the geometry but also the properties of the edge. Experimental results show that a drag finished edge has the lowest edge surface roughness ( $R_a = 0.42 \mu\text{m}$ ), while abrasive jet machining can induce 63% greater compressive residual stress than the unprepared tool. Reduction in tool wear was observed at the same stage of cutting length in the prepared edges alongside improved edge hardness. A thermomechanical finite element analysis is performed to evaluate the thermomechanical behavior of all the cutting edges. Results demonstrate that the use of prepared cutting edges enhances stress distribution and reduces the temperature. Experimental results confirm that the drag finished edge has the best overall performance out of the three edge techniques with lower cutting temperature, better stress distribution, lower cutting forces, reduced flank wear, and reduced roughness of the machined surface finish.

**Keywords** Cutting edge preparation · Wet abrasive jet machining · Brushing · Drag finishing · Tool life

## 1 Introduction

Development of modern cutting tools consists of four essential related aspects: tool substrate material, coating technology, tool macro geometry, and cutting edge preparation techniques [1]. Research studies on cutting edge preparation have become more frequent in the last decade, due to its low cost and high impact on the machining process. In addition, the economic aspects of manufacturing are under higher levels of scrutiny as well [1]. One of the fundamental objectives of an economically efficient machining process is to minimize the cost of the tool and its replacement. Generally, edge preparation techniques require a lower initial investment and operating cost compared to other manufacturing processes used to produce high-quality-coated cutting tools.

Edge preparation modifies the local macro and micro-geometry of a tool's sharp edge, removing initial edge defects by replacing them with a smooth profile, thereby increasing the tool quality. Furthermore, the purpose of cutting-edge preparation is to create a cutting edge that possesses better stability, reduced edge chipping, and improved tool surface

---

✉ A. F. M. Arif  
afmarif@mcmaster.ca

Wanting Wang  
wangw80@mcmaster.ca

Md Khalid Saifullah  
saifulm@mcmaster.ca

Robert Aßmuth  
robert.assmuth@tu-dortmund.de

Dirk Biermann  
dirk.biermann@tu-dortmund.de

S. C. Veldhuis  
eldhu@mcmaster.ca

<sup>1</sup> Department of Mechanical Engineering, McMaster Manufacturing Research Institute (MMRI), McMaster University, 1280 Main Street West, Hamilton, ON L8S4L7, Canada

<sup>2</sup> Institute of Machining Technology, Technische Universität Dortmund, Baroper Straße 303, 44227 Dortmund, Germany

integrity, all of which further enhance the chip flow process and cutting action. As a result, tool life and process reliability are improved while tool wear rate is decreased, thus achieving an overall better workpiece [2, 3].

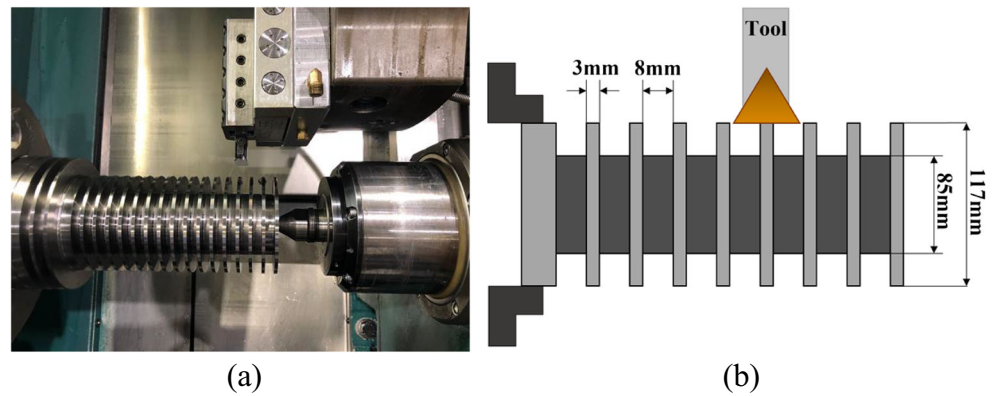
To avoid unpredictable cutting-edge chipping and to improve the quality of the machined surfaces [4], careful selection of edge preparation techniques should be made. Appropriate choice of cutting tool edge preparation techniques depend on their area of application and productivity. Currently, the most common preparation methods are grinding [4, 5], dry and wet abrasive jet machining [6–10], brushing [11, 12], and drag finishing [13, 14]. Other techniques under development include magneto abrasive machining and electrical discharge machining (EDM) [15].

Wet abrasive jet machining (WAJM) is an edge preparation process that removes material from the sharp tip of the tool through an erosion mechanism. It requires an abrasive medium mixed in a carrier medium, which is then sprayed on the cutting tool surface via a jet nozzle. This kind of machining is distinguished by the type of medium used in the process. Dry abrasive jet machining uses air for this task whereas water is used in wet abrasive jet machining. Several studies reported the influence of wet abrasive jet machining on the produced cutting tool [9, 16]. The most obvious advantage of abrasive jet machining is its ability to induce compressive stress within the tool edge surface and the subsurface of PVD-coated tools, which enhances toughness and reliability of the cutting edge as well as the superficial film strength properties of the PVD coating. It was reported that wet abrasive jet machining can generate surfaces with lower roughness compared to dry abrasive jet machining due to the buffering and damping effect of the liquid carrier medium that produces minimal thermally induced distortions on the machined surface. In addition, water can also suppress dust in the process, reducing negative health issues associated with air-borne particles [3]. Krebs et al. [9] demonstrated that abrasive jet machining has the capability to prepare micro milling tools with high efficiency. An impact time of only approximately 1 min was needed to produce a rounded edge with 20  $\mu\text{m}$  average cutting-edge rounding.

Brushing is widely used to remove material for setting different cutting edge rounding sizes, as well as in surface treatments and the deburring process [11]. When a defined edge is rounded by brushing, the inserts are passed through rotating abrasive brushes. In some applications, inserts also rotate around the machine table as they revolve under the brushes [15]. The brush forms are usually wheels, disk brushes, cup brushes, and wire end brushes. Different types of brush filaments and different process parameters can produce various edge radii ranging from a few microns to tens of microns [11]. Depending on the application, the abrasive brush is mounted with bristles or filaments of extruded polymer fibers such as nylon or wire that contain an abrasive material such as silicon carbide (SiC), aluminum oxide (Al<sub>2</sub>O<sub>3</sub>), cubic boron

nitride (CBN), and polycrystalline diamond (PCD) [17]. The morphology of the generated surface may vary with the application of different brush materials, paths taken by the brush, and process conditions like speed and rotation direction. A distinctive advantage of brushing is the ability to produce a rounded cutting edge in a short time. With its high rate of material removal, brushing is recognized to be a highly effective method that is applicable to a wide range of cutting tool materials. Following continuous development in brushing edge preparation technology, a modern 5-axis machine can produce complex cutting edge geometries associated with a wide range of different cutting tools. In drag finishing, the cutting tools are immersed in a container, with abrasive particles. The tools rotate inside the container and the material on the tool edge can be removed by the continuous abrasion of the tool edge surface by abrasive particles. A homogeneous cutting edge rounding of a complicated tool edge profile can be achieved with this method. In addition, it is possible to obtain reliable honed cutting edges that have a precisely defined radius with high productivity at a relatively low cost. Also, the drag finishing process could reduce binder material (which is Cobalt in this study) leaching. The equipment used in the drag finishing process may consist of either one or two containers with different kinds of abrasive media inside. Different media can meet different requirements of edge preparation and polishing such as roughing and fine polishing. It is worth noting that diverse media should be applied to produce a honing edge at a range of various edge radii, which are usually silicon carbide, ceramic, quartz, or plastic bonded abrasive particles. As for edge preparation, commonly used abrasive media types are HSC, H3, and H4. Some of the process parameters are controlled during the process, since they can influence the edge microgeometry and tool surface quality. A literature review by Uhlmann et al. reported that abrasive medium specifications, rotational speed, immersion depth, rotation direction, and machining time are the main influencing factors of the prepared edge geometry [14].

Although the influence of different edge preparation technologies on tool performance during the turning process has been investigated, there is a scarcity on comparative studies in the literature. Bouzakis et al. [10, 18] demonstrated that the wear behavior of the coated cutting edge radii manufactured by grinding is significantly superior to that of the micro-blasting preparation method. In a ground edge, the first coating fracture appears after  $2 \times 10^4$  cuts, which is much later than in the corresponding micro-blasted edges. In 2014, Denkena et al. [5] investigated the influence of plunge-face grinding and brushing on the performance of coated tungsten carbide inserts during hard turning. The results revealed that the compressive residual stresses induced in the cutting edge by brushing were higher than those induced by grinding. Cutting forces in the brushed inserts were about 10% lower than in the ground inserts. Fulemova et al. [13] prepared the cutting insert edge using different technologies and reported

**Fig. 1** a Machining setup. b Workpiece

that at the same edge radius value, the tool treated with drag finishing had the longest tool life whereas the tool that underwent laser machining had the shortest tool life. Additionally, drag finishing enhances the cutting tool life by about 60% compared to a tool that was treated only by grinding.

There are two main approaches to studying the prepared cutting tool thermal and mechanical behavior—experimental and finite element analysis (FEA). Yen et al. [19] conducted a finite element analysis of process variables (temperature, stress, and strain) in orthogonal machining using different tool edge geometries. Their results show that the maximum tool temperature is lower when the edge radius is equal to 0.05 mm (compared to 0.01 mm and 0.1 mm edge radius). However, the average tool-chip interface temperature monotonically increases along with edge radius. Both the highest normal stress and shear stress along the rake face occur near the tool-tip. Strain in the secondary shear zone increases considerably along with edge radius due to greater plastic deformation. Özel and Zeren [20] applied FEA to simulate the orthogonal machining of AISI 4340 steel with round carbide edge cutting tools. A higher temperature was predicted at greater depths of cut and with larger edge radius tools. Moreover, as the tool edge roundness increases, the machining-induced residual stresses also rise in the workpiece surface.

Many studies emphasized the influence that edge geometries have on cutting forces and tool wear mechanisms. The mainstream opinion is that different edge radius values variously contribute to the cutting process. However, the different preparing processes that generate rounded or chamfered cutting edges also play an important role, which needs to be

studied in greater detail. Limited research has been performed on the properties and quality of the cutting edge, as well as the underlying methods of edge preparation and their influence on the edge properties. Consequently, this paper presents the results of a comparative study of three edge preparation technologies: AJM, brushing, and drag finishing. First, a detailed investigation of cutting edges prepared by different methods is presented. Next, the orthogonal finish turning of AISI 4140 alloy steel is carried out to evaluate and compare its performance in terms of tool life and machined surface quality. Finally, finite element analysis was performed to investigate the role of the thermomechanical behavior on the performance of the prepared edges.

## 2 Experimental work

### 2.1 Experimental procedure

Figure 1 a shows the experimental setup of the tests in this study. A Nakamura-Tome SC-450 super multitasking turning machine was used to perform a series of orthogonal turning tests with a connected KISTLER dynamometer to collect the cutting force data. AISI 4140 steel with 32 HRC hardness served as the workpiece material. The experiment setup for the grooving process on the front view is shown in Fig. 1b. The chemical composition of the workpiece is given in Table 1. The cutting insert was an uncoated TPG 322 cemented carbide of grade K313 with 6% Co, supplied by Kennametal. The machining test was performed at a feed rate of 0.1 mm/rev and depth of cut of 3 mm. The cutting speed

**Table 1** Chemical composition and mechanical properties of AISI 4140 steel [21]

Chemical composition (%)							
C	Si	Mn	P	S	Cr	Ni	Mo
0.38–0.43	0.15–0.32	0.75–1.00	Max 0.035	0.04	0.80–1.08	0.16	0.15–0.25

**Table 2** Material properties of the AISI 4140 workpiece and the uncoated carbide tool [21, 22]

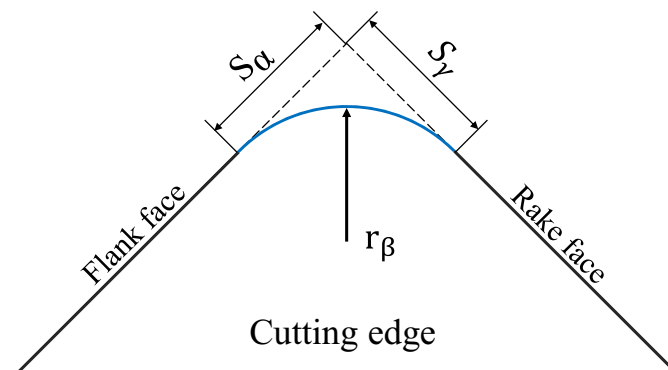
Material parameter	Units	Workpiece (AISI 4140)	Cutting tool (uncoated carbide)
Density	Kg/m <sup>3</sup>	7800	15,290
Young's modulus, E	GPa	210	705
Poisson's ratio, $\nu$	–	0.3	0.23
Yield strength	MPa	415	
Tensile strength	MPa	655	
Hardness		31 HRC	
Specific heat capacity	J/kg <sup>°</sup> K	473@200 °C 519@ 400 °C 561@600 °C	178
Thermal expansion coefficient, $\alpha$	mm/m <sup>°</sup> K	12.2 @ 20 °C 13.7 @ 250 °C 14.6 @ 500 °C	7.1
Thermal conductivity	W/m <sup>°</sup> K	42.6 @ 20 °C 42.3 @ 200 °C 37.7 @ 400 °C 33.0 @ 600 °C	24
Melting temperature, $T_m$	°K	1793	2800
Bulk Temperature, $T_r$	°K	300	300

was 300 m/min. It should be mentioned that the K313 insert is not recommended by the supplier for the purpose of cutting 4140 steel. However, from an academic perspective, the main objective of this study is to investigate the different behaviors of prepared and unprepared inserts and highlight the effects of the edge preparation process. Therefore, inserts made from this material were used in the current study to accelerate the tool wear rate and save workpiece materials.

The general thermal and mechanical properties of the workpiece and the cutting tool are given in Table 2. These properties are used in material modeling for numerical work. The specific heat of the workpiece material is highly temperature dependent since the material undergoes a phase change at about 1000°K. Therefore, temperature-dependent specific heat capacity is used in the workpiece according to [23].

The methodology and equipment used to achieve the proposed objectives are presented. Cutting edge geometry is

characterized by microgeometry and edge surface topography in this study. Alicona Infinite Focus 3D measurement system is used to observe and measure the tool edge micro-geometries obtained by brushing, drag finishing, and wet abrasive jet machining. All the measurements were repeated more than six times to guarantee repeatability and accuracy. The quality of the produced cutting edges was investigated using a JEOL 6610LV scanning electron microscope (SEM). The surface roughness parameter  $Ra$  was measured at different positions along the edge surface near the cutting edges and on the rake face of the tools using an Alicona infinite Focus system. The residual stresses on the edge surface were measured at the intersection of the rake face and the cutting edge by Bruker's X-ray Diffraction 3 system, with 1.79026 Å wavelengths of Co radiation. The measurements were then analyzed by LEPTOS software using normal load. The hardness of different inserts was measured with an Anton Paar

**Fig. 2** Form-factor method and the parameters used in edge geometry determination

where,

$S_\gamma$ : Cutting edge segment on the rake face

$S_\alpha$ : Cutting edge segment on the flank face

$K$ : Form factor or K-factor

$\bar{S}$ : Average cutting-edge rounding

$$K = \frac{S_\gamma}{S_\alpha} \quad \text{and} \quad \bar{S} = \frac{S_\alpha + S_\gamma}{2}$$

$r_\beta$ : Average cutting-edge radius

**Table 3** Wet abrasive jet machining parameters

Abrasive medium	ZWSK 220, aluminum oxide ( $\text{Al}_2\text{O}_3$ ), blocky
Average grain size	58 $\mu\text{m}$
Hardness	21 $\text{kN/mm}^2$
Density	3.96 $\text{g/cm}^3$
Melting point	2050 $^\circ\text{C}$

Nanoindentation Tester (NHT<sup>3</sup>) and analyzed using Indentation Software Version 8. Vickers hardness (expressed by the symbol HV) was used in the test. The NHT<sup>3</sup> indenter can deliver a load ranging from 0.1 to 500 mN. Depending on the cutting tool material, 100 mN was suggested to be applied for all inserts in this study.

During a series of turning tests, tool flank wear width progress was measured by a Keyence digital optical microscope (VHX 5000) after each cutting length of around 1500–1900 mm. The cutting tool was also examined by SEM to investigate the cutting-edge wear mechanisms, combined with energy-dispersive X-ray spectroscopy (EDS) to examine the wear-acting mechanisms on the flank and rake faces of the cutting tools. The roughness of the machined AISI 4140 steel surface was measured with a Mitutoyo SJ-201 profile tester after being cut by different types of cutting edges. Moreover, the cutting forces in the cutting and feed directions were monitored for each cutting test by a KISTLER dynamometer for the first 8000 mm.

## 2.2 Sample preparation

The size and shape of the cutting edge were characterized in this study by the form-factor method shown in Fig. 2. In order to assess the effect of edge preparation methods on cutting tool performance, samples with three different preparation processes, wet abrasive jet machining (WAJM), brushing (B), and drag finishing (DF), were prepared for a same  $\bar{S}$  value

with  $K = 1$  (symmetric). The unprepared edge of the as-received insert was used as the benchmark.

The cutting-edge samples were prepared by wet abrasive jet machining in collaboration with Institute of Machining Technology, TU Dortmund University using a Restec GmbH Nicolis Technology machine type WA 110-P with 6-axis robot control. A jet pressure ( $P_{st}$ ) of 5 bar and the nozzle distance ( $h_d$ ) of 20 mm were constantly held throughout the edge preparation process. Different jet feed speeds ( $v_{f, st}$ ) and different relative jet inclination angles ( $\alpha_{st}$ ) were applied to produce different edge geometries. The data regarding abrasive media and process parameters are given in Table 3.

Brushing samples were prepared by a SAACKE 5-axis CNC Machining Center, which can reprocess and manufacture HSS and carbide tools with five fully controlled axes. Figure 3 shows the process setup and parameters. Drag finishing samples were prepared with a DF35 machine manufactured by OTEC PR ZISIONSFINISH GMBH, Straubenhardt, Germany. The rotational speed and direction could be controlled by the machine's motors. The DF35 machine, abrasive media, and process parameters suitable for generating the desired edge rounding are given in Fig. 4. Figure 4 b shows the images of HSC 1/300 and H4 1/400 abrasive media taken from SEM. The walnut shell granulates above the red line are the H4 1/400 media, whereas the walnut shell granulates under the red line are the HSC 1/300 media. Abrasive media HSC 1/300 is used to prepare an edge rounding of up to 30  $\mu\text{m}$  in this study.

## 2.3 Results and discussion

The results of cutting-edge characterization, tool life, and tool wear analysis, together with machined surface quality evaluation, are presented from the comparison view in this section.

### 2.3.1 Cutting edge characterization

The target geometry of the prepared edge was symmetric ( $K = 1$ ) with  $\bar{S} = 20 \mu\text{m}$ . The edge geometry of all unprepared and

**Fig. 3** Brushing machining **a** setup and **b** brush



(a)



(b)

#### **Process parameters:**

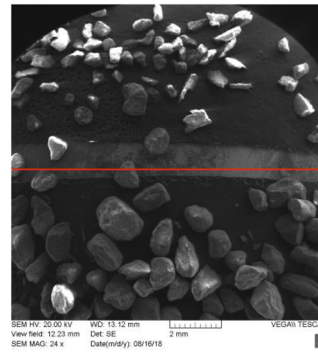
Rotation speed = 2000 rpm,  
In-feed (depth in brush) = 0.8mm,  
Brush time = 1 sec,  
Grit size = 2000,  
Brush type = Nylon with diamond abrasive on the ends.



**Fig. 4** Drag finishing **a** machine and **b** HSC 1/300 and H4 1/400 abrasive media



(a)



(b)

**Process parameters:**

Rotation speed = 40 rpm,  
 Depth in media = 50 mm,  
 Processing time = 10 min\*,  
 Abrasive media = HSC /300,  
 \* Tool rotates 5 minutes left (toward the rake face) and 8 minutes right (toward the flank face), based on several trials and tests.

prepared inserts was measured using an Alicona Infinite Focus microscope with the data recorded in Table 4, and real shape of the cutting-edge geometry is shown in Fig. 5. All three techniques were shown to be able to produce a rounded edge within an acceptable range of accuracy. Since the sample size is not enough to tell the trend of variation trend between the targeted and measured values of each method, results can only confirm that the wet abrasive jet machined edges have a smaller tolerance for every parameter, compared with the other two methods.

Edge topography describes the surface structure of the cutting edge. As mentioned before, new sharp cutting inserts without edge preparation involve typical edge defects in the edge region, such as micro-breakages, burrs, bad surface finish, and irregularities along the edge [24]. Furthermore, the grinding marks generate a serrated texture near the cutting edge. All these edge defects lead to a large deviation in measurement along the cutting edges and cause chatter during the cutting process, consequently reducing stability. Figure 6 shows SEM images of major surface defects in the cutting-edge region of the as-received unprepared inserts.

Scanning electron microscopic (SEM) pictures in Fig. 7 show the cutting-edge topographies prepared by three different methods. However, the abrasive jet machined cutting edge in Fig. 7a has more dimple structure area near the cutting edge

compared to the other two cutting edges, which makes the edge surface appear less smooth. Figure 7 b shows that the brushed inserts have less breakage and chipping on the edge surfaces and that the grinding texture was partly removed. However, the edge rounding is not perfectly smooth; there are still some undulations and unevenness on the edge surface because each bristle is not the same and irregularities exist in the brush material. It is extremely difficult to produce an extremely uniform surface during such a short contact time (one second in Fig. 3). The cutting-edge region of the drag finishing prepared insert was effectively honed by granulates and the edge itself has a uniform and smooth surface, as shown in Fig. 7c. However, the intersection of the cutting edge and flank face is not very smooth, and a rib is located slightly below the top of the rounded edge.

Surface roughness was measured on the cutting-edge area and the tool rake face. The arithmetical mean deviation of the profile surface ( $Ra$ ) is used to evaluate the overall finish condition of a surface. Measurements were taken parallel to the cutting edge to assess the extent of chipping along it. All measurements on the tool rake face were made perpendicular to the edge, which corresponds to the direction of chip flow in orthogonal cutting.

Figure 8 a shows that the wet abrasive jet machined edge surface roughness ( $Ra$  value) is about 91% higher than in the

**Table 4** Measured form-factor parameters of cutting tool sample edges

Edge condition		Measurement parameters		
		K	$\bar{S}$ ( $\mu\text{m}$ )	$r_{\beta}$ ( $\mu\text{m}$ )
Unprepared edge	U	$1.20 \pm 0.110$	$4.69 \pm 0.23$	$3.61 \pm 0.16$
Wet abrasive jet machining	WAJM	$1.08 \pm 0.012$	$27.26 \pm 0.26$	$21.89 \pm 0.29$
Brushing	B	$1.18 \pm 0.040$	$28.38 \pm 0.78$	$19.33 \pm 0.44$
Drag finishing	DF	$1.12 \pm 0.030$	$25.02 \pm 0.68$	$20.82 \pm 0.69$

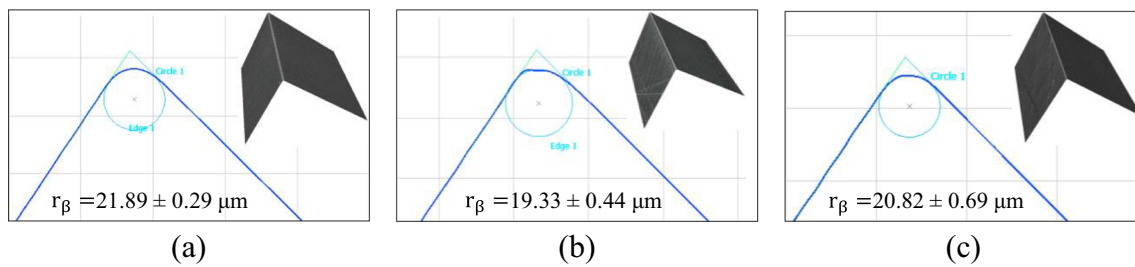


**Fig. 5** Real shape of the cutting-edge geometry prepared by **a** wet abrasive jet machining, **b** brush, and **c** drag finish, measured by Alicona Infinite Focus 3D measurement system

unprepared edge. A roughness reduction of about 22% and 38.6% is observed in edges prepared by brushing and drag finishing, respectively. A similar trend applies to the rake-face roughness (Fig. 8b). Abrasive jet machining generates 15% more, brushing 35% less, and drag finishing 49% less roughness than the unprepared edge. In conclusion, wet abrasive jet machining provides better control of micro-geometry shape and size but results in higher surface roughness. On the other hand, drag finish gives the smoothest surface in comparison to other methods of surface preparation. These findings are consistent with the observations of edge topography as discussed for various edges. A study by C. Rodríguez [1] and K. D. Bouzakis et al. [10] shows that aluminum-oxide particles carried by pressurized water jet impact on the edge surface in WAJM causes a reduction in binder material and may cause carbide removal, which results in a rougher surface. In contrast, brushing and drag finishing do not involve high-pressure impact and thus produce a smoother surface.

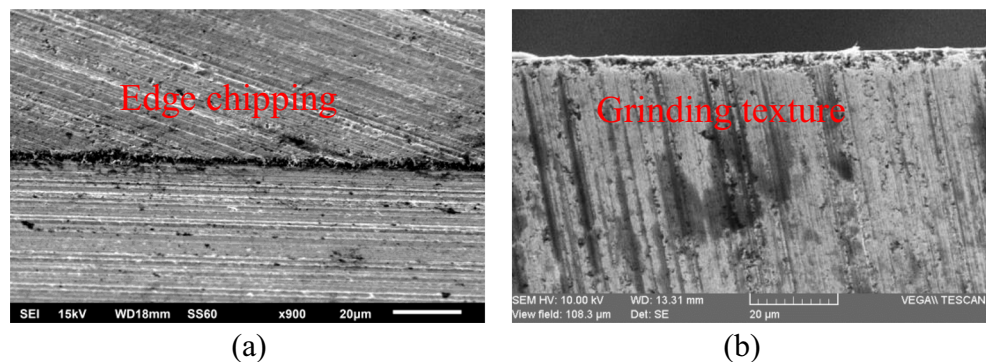
In wet abrasive jet machining, the mechanical load comes from the aluminum-oxide particles which are used to remove the material from the sharp tool tip. Plastic deformation of the cutting-edge surface is induced to compel the underlying material to resist this deformation and retain its initial form, which generates compressive surface stress. Aluminum-oxide particles impact the edge surface during the WAJM process causing plastic deformation on the edge surface. Strain hardening may happen and, therefore, influence the hardness of the cutting-edge area. During the brushing

process, the filaments of the brush generate mechanical loads on the cutting-edge surface. The rotation motion of the brush responsible for removing material from the sharp tool tip creates plastic deformation in the edge surface material. Compressive surface stress is therefore induced so that the underlying material would maintain a static equilibrium state. During the drag finishing treatment, cutting tools are immersed and abraded in a filled with abrasive particles. The impact between the abrasive media and the cutting tool will cause plastic deformation of the edge surface material, thereby inducing residual stresses into it. Since the rotation speed of this process is relatively low, almost no thermal load acts on the cutting edge which may generate tensile residual stress.

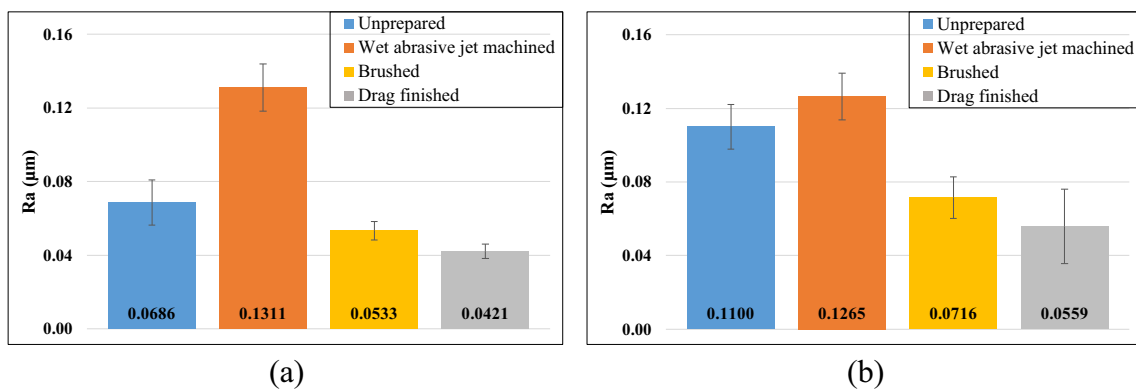
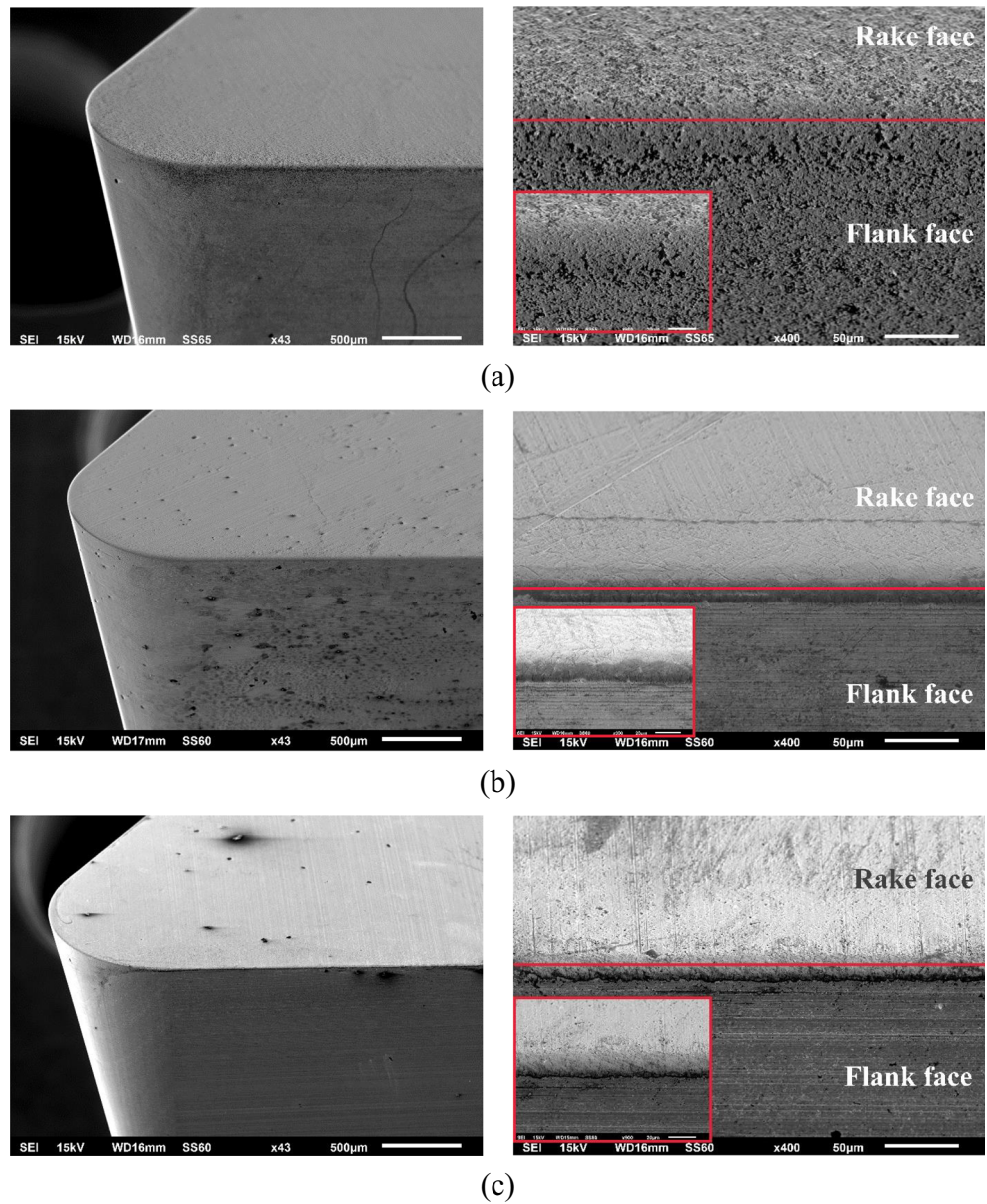
Table 5 shows that the compressive residual stress is higher in the prepared edges than in the unprepared edge. But the WAJM sample has the greatest compressive stress, 62.7% greater than the unprepared edge. Since the aluminum-oxide particles in WAJM are driven by pressure and worked through a nozzle from a certain distance range, the kinetic energy carried by the particles is much greater than that carried by the brush and the walnut shell granulate to the edge surface in brushing and drag finishing, respectively. Therefore, the impact of abrasive particles induces higher compressive residual stress.

Table 5 also shows that the prepared cutting edges have a higher hardness than previously. The hardness (HV value) of the three types of prepared edges are almost at the same level, but the error bar of the hardness of abrasive jet machined

**Fig. 6** SEM images showing defects in the cutting-edge region of the as-received unprepared inserts, **a** edge chipping and **b** grinding texture



**Fig. 7** SEM images of the cutting edge prepared by **a** WAJM, **b** brushing, and **c** drag finishing



**Fig. 8** Comparison results of surface roughness ( $R_a$ ) between prepared inserts and unprepared inserts on **a** cutting edge area and **b** rake face



**Table 5** Compressive residual stress and hardness measurements for different edges

Types of edge Measurement	Unprepared edge	Wet abrasive jet machined edge	Brushed edge	Drag finished edge
Compressive residual stress	1140.2 ± 46.0	1877.7 ± 37.7	1193.1 ± 58.6	1327.5 ± 49.8
Hardness	1679.6 ± 46.9	2201.6 ± 302.4	2337.1 ± 164.9	2368.6 ± 65.4

edges is quite higher than that of the other three tested edges. The same instrument was used to conduct all of the nano-indentation tests, indicating that the WAJM produced surface is not very smooth, which results in this variation.

**2.3.2 Tool life analysis**

The results of the tool life study are presented in this section. First, a set of tool life tests were performed using uncoated unprepared tungsten carbide inserts as the benchmark. Next, machining tests were conducted for all inserts with differently prepared edges and their performance was compared with that of the unprepared benchmark tool. During these orthogonal turning tests, maximum tool flank wear was monitored and measured after each pass (lengths of the cut was around 1500 mm to 2000 mm) using a Keyence VHX-500 digital microscope.

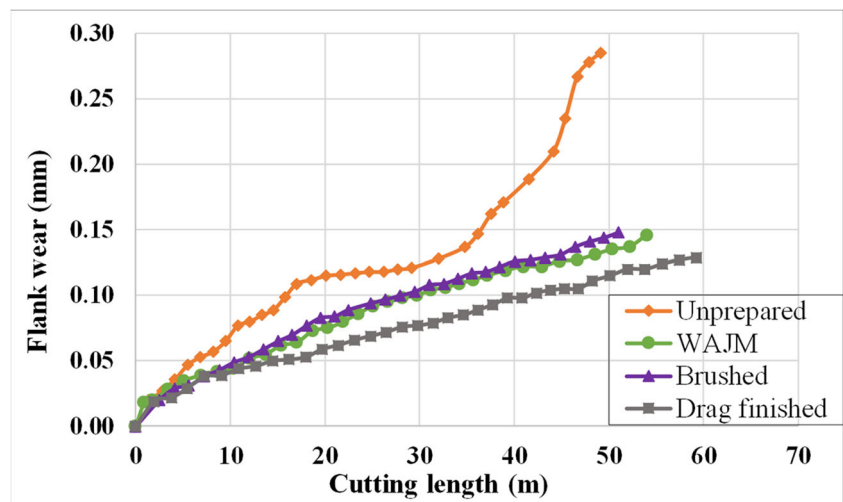
Figure 9 shows the tool life test results for inserts prepared by WAJM, brushing, and drag finishing in comparison to the unprepared cutting edge. Prepared edges performed better till failure with lower flank wear value and more gradual wear growth trend, comparing with the benchmarked tool. Figure 10 compares the cutting length at 100 μm and 120 μm flank wear. Results show that all of the prepared edges were capable of extending the tool life to a greater extent than the unprepared edge. The abrasive jet machined inserts, brushed inserts, and drag finished inserts can improve tool life

by 97.6%, 77.0%, and 167.8% respectively, at a 100-μm maximum flank wear. At 120 μm, the tool life enhancements achieved by these three kinds of prepared inserts are 48.1%, 39.0%, and 94.5% respectively. The drag finished edge shows the best performance.

The reason why edge preparation can extend the life and reduce wear is that it strengthens the cutting edge during the preparation treatment. In pictures taken by the Keyence VX-5000 microscope (Fig. 11), no major edge chipping was found in all the prepared inserts prior to the flank wear width reaching 120 μm. In contrast, the first chipping occurred quite early in the unprepared inserts (flank wear = 27 μm, cutting length = 2792 mm). Some slight chipping was found on the abrasive jet machined edge when the cutting length exceeded 12 m, but after four passes, most of the edge chipping disappeared through rubbing. It could be demonstrated that no matter the process, edge preparation can provide much better stability to the cutting edge.

Figure 12 shows the influence of edge preparation on the cutting force components. Force comparison shows that all of the prepared edges generate higher cutting and feed forces than the unprepared edge. The increase in cutting forces is not as great as the increase in feed forces. As previous studies have shown [25], force components should increase on the edge with greater average edge rounding as it is more difficult for the blunt cutting edge to remove material from the work-piece. In addition, the feed force is more pronounced than the

**Fig. 9** Effect of three different edge preparation techniques on tool life



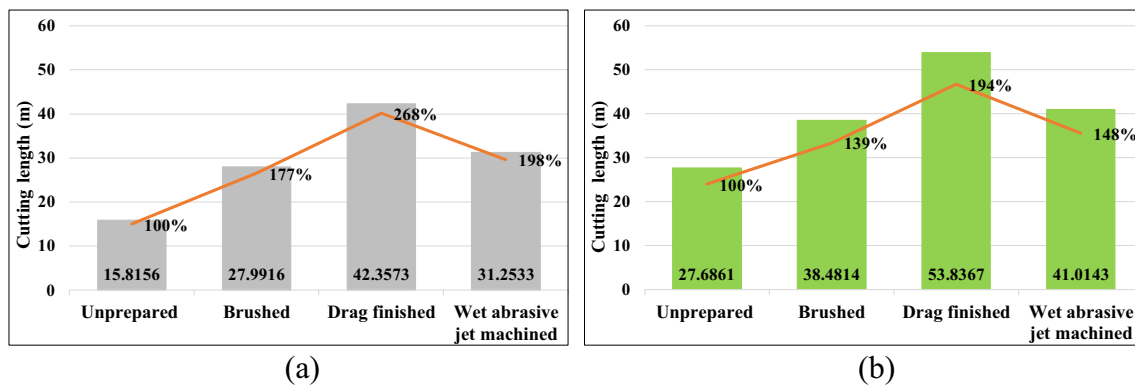


**Fig. 10** Tool life comparison at **a** 100  $\mu\text{m}$  flank wear and **b** 120  $\mu\text{m}$  flank wear

cutting force, since abrasion wear on the flank face has a greater influence on the motion in the feed direction [1, 26]. The cutting force of the drag finished edge is almost the same as that of the unprepared one. Feed force growth is not as high in the brushed inserts and abrasive jet-machined inserts. Lower cutting forces are observed in drag finishing, which is consistent with the edge roughness and hardness measurements in Table 5 as well as tool life results in Fig. 10. Thus, it implies that the tools with better edge surface finish can reduce cutting forces, thereby maintaining their cutting capability for a longer time.

To clearly show the combined effects of edge preparation, a global Table 6 with all data is shown below:

### 2.3.3 Surface roughness of the workpiece

Figure 13 illustrates the surface roughness of the AISI 4140 workpiece following orthogonal turning using tools with unprepared and different prepared edges. All roughness measurements were made by a Mitutoyo SJ-201 profile tester. The data show that all of the prepared cutting edges deliver a better surface finish compared to the unprepared cutting-edge, with a  $R_a$  of 0.45  $\mu\text{m}$ . The best surface finish at a  $R_a$  of 0.27  $\mu\text{m}$  occurs when drag finishing is used to produce edge rounding. Since the average edge rounding of the three prepared edges are almost the same, the edges have comparable contact area with the workpiece. The edge with the best

edge surface (drag-finished edge) (refer Fig. 8) can contribute to the smoother machined surface due to less friction and lower tool flank wear.

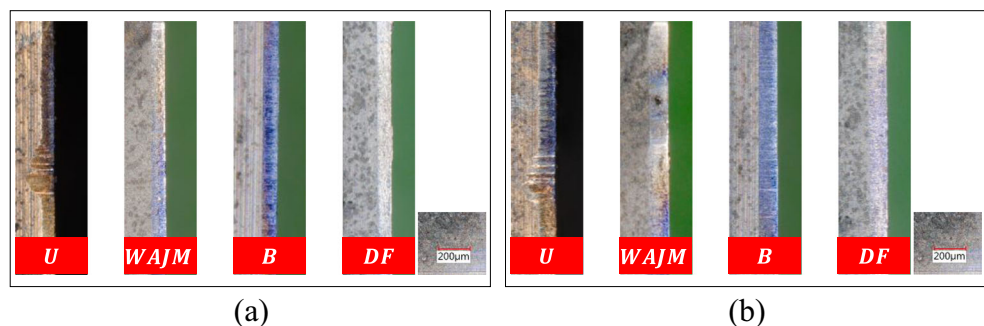
## 2.4 Numerical work

The thermomechanical behavior at the tool-workpiece interface during the machining process directly affects the tool performance and the quality of the machined surface. However, due to the complexity and the restricted accessibility, the determination of temperature and stress distribution using an accurate and convenient method remains challenging. Finite element modeling is one of the most effective ways to predict the thermomechanical properties. In this section, the variation in the thermomechanical behavior of different prepared edges has been numerically investigated. For this purpose, a fully coupled finite element analysis is carried out in the current study to evaluate the thermomechanical behavior of prepared edges using ABAQUS/EXPLICIT commercial FE software. An Arbitrary Eulerian-Lagrangian (ALE) method with an activated adaptive meshing capability is used in the numerical simulation of the orthogonal machining process.

### 2.4.1 Finite element model

Figure 14 shows the geometric model and boundary conditions used in the current work. For ALE analysis shown

**Fig. 11** Edge flank wear observation measured on a flank wear width of **a** 84  $\mu\text{m}$  and **b** 120  $\mu\text{m}$



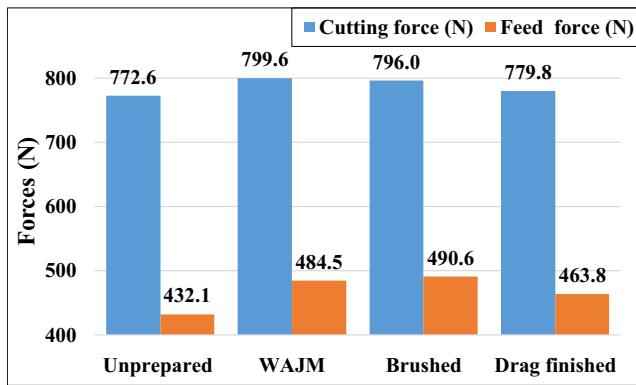


Fig. 12 Comparison of cutting force components

in Fig. 14, the workpiece is fixed in the y-direction, moving in the x-direction only at the prescribed cutting speed. The cutting tool is fully constrained. The workpiece length was set to be 5 mm and height to 2 mm. The uncut chip thickness is 1 mm. The same tool geometry and cutting speed as in the experimental study was used in all the simulations. A plain strain, quadrilateral, linearly interpolated, and thermally coupled (CPE4RT) element was used for finite element discretization. Mesh convergence was performed to achieve a balance between force prediction accuracy and computation time, with the mesh refinement mainly being in the three shear deformation zones (primary, secondary, and tertiary).

The metal removal process involves very large plastic deformation with a very high strain rate and temperature. The Johnson-Cook material model of Eq. (1) is used in this work, which is the most common constitutive relationship in metal cutting simulations.

$$\bar{\sigma} = \left[ A + B \bar{\epsilon}_p^n \right] \left[ 1 + C \ln \left( \frac{\dot{\bar{\epsilon}}_p}{\dot{\bar{\epsilon}}_0} \right) \right] \left[ 1 - \left( \frac{T - T_r}{T_m - T_r} \right)^m \right] \quad (1)$$

where

- $\sigma_{eq}$  equivalent plastic flow stress.
- A initial plastic flow (yield) stress
- B coefficient of strain hardening

- N strain hardening exponent
- C strain rate dependency coefficient
- $\bar{\epsilon}_p$  equivalent plastic strain
- m thermal softening index
- $\dot{\bar{\epsilon}}_p$  equivalent plastic strain rate
- $\dot{\bar{\epsilon}}_0$  reference plastic strain rate
- T current temperature
- $T_r$  room temperature
- $T_m$  melting temperature

The workpiece was AISI 4140 steel, and the modeled cutting tool was made of cemented carbide. The Johnson-Cook parameter values used to simulate the behavior of the AISI 4140 workpiece are specified in Table 7.

The source of temperature in metal cutting between the tool and the workpiece is plastic deformation and friction. In the thermal interaction between the tool and chip interface, the generated heat flux is

$$q_f = \eta_f \tau_f \left( \frac{\Delta S}{\Delta t} \right) \quad (2)$$

where  $\Delta S$  is the incremental slip at the tool-chip interface at a time segment  $\Delta t$  and  $\tau_f$  is frictional stress [27].  $\eta_f$  is the portion of energy produced during the frictional slip that is converted to heat. The value  $\eta_f$  was reported to be between 0.85 and 1 in the literature [28]. An  $\eta_f = 0.9$  is used for all the simulations in this study. The gap conductivity between the workpiece and the cutting tool was assumed to be  $1000 \text{ W/m}^2/\text{°C}$  according to the literature [29]. A combination of Coulomb’s and a shear friction model is used to model the interaction at the tool-workpiece contact as given in Eq. (3). Based on pin-on disk experimental results, the coefficient of friction between the uncoated carbide and 4140 steel can vary from 0.2 to 0.6 [30]. In this study, a COF of 0.4 is used for all the numerical analyses.

$$\tau_f = \min(\mu \sigma_n, \tau_y) \quad (3)$$

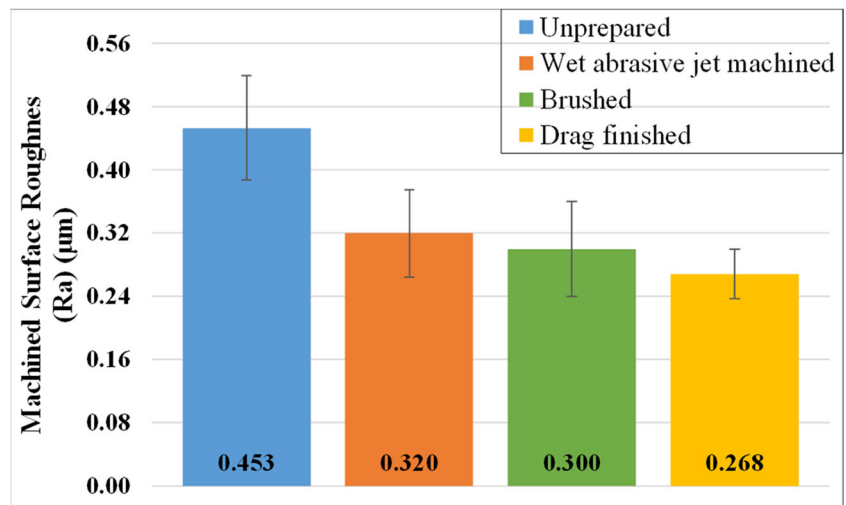
where,

- $\tau_f$  frictional stress

Table 6 Comparison of effects of three different edge preparation methods

Edge preparation techniques	Edge surface roughness ( $\mu\text{m}$ )	Hardness (HV)	Compressive residual stress (MPa)	Tool life at flank wear = $100 \mu\text{m}$ (%)	Cutting force (N)
Unprepared	0.0686	$1140.2 \pm 46.0$	$1679.6 \pm 46.9$	100%	772.6
Wet abrasive jet machining	0.1311	$2201.6 \pm 302.4$	$1877.7 \pm 37.7$	198%	799.6
Brushing	0.0533	$2337.1 \pm 164.9$	$1193.1 \pm 58.6$	177%	796.0
Drag finish	0.0421	$2368.6 \pm 65.4$	$1327.5 \pm 49.8$	268%	779.8

**Fig. 13** Machined surface roughness measurements



- $\mu$  coefficient of friction  
 $\sigma_n$  normal stress  
 $\tau_f$  limiting shear stress ( $= \frac{\sigma_y}{\sqrt{3}}$ )  
 $\sigma_y$  uniaxial yield stress

The prediction of worn tool geometry has always been challenging. In the previous studies, either tool geometry was predicted based on nodal displacement or assuming displacement vector parallel to the machined surface at the tool tip [31, 32]. Both approaches have computational limitations such as mesh convergence and less realistic worn tool geometry. On the other hand, Keyvan et al. directly exported worn tool geometry from the experimental study where the worn cutting edge resembles a chamfered edge [33].

Since the prediction of tool wear was not the objective of this numerical study as described in the introduction of this section, a computationally simplified modeling approach was adopted by using experimentally measured flank wear from Fig. 9 for different edges to model worn tool geometry. For this purpose, a simpler but novel approach was employed to update the cutting edge by introducing a tangent at the flank edge. First, the flank edge was determined based on sign of friction stress from simulation results as described in Fig. 15a.

Next, considering the flank edge as an arc, a tangent was drawn at the midpoint, as shown in Fig. 15b. Once the tangent line was defined, it was displaced in the normal direction based on the experimental flank wear (Fig. 9). The tangent makes an inclination angle ( $\beta$ ) with respect to the machined surface. This inclination angle depends on the micro-geometry of the cutting edge and varies for different prepared edges.

## 2.4.2 Numerical results

The results of numerical simulations describing the thermomechanical behavior of tool with initial edge and its progression as it wears out are discussed in this section.

The variation in the maximum temperature due to progression of wear on the flank face for four different edges is shown in Fig. 16. At the initial stage of wear, the maximum temperature on the flank face is the same for all the edges. However, as tool wear increases, the maximum temperature also increases in all the cutting edges. The growth of maximum temperature in the unprepared cutting tool is higher than that of prepared tools. The maximum temperature of the unprepared cutting tool increases by up to 70% after a cutting length of

**Fig. 14** ALE model for machining simulation

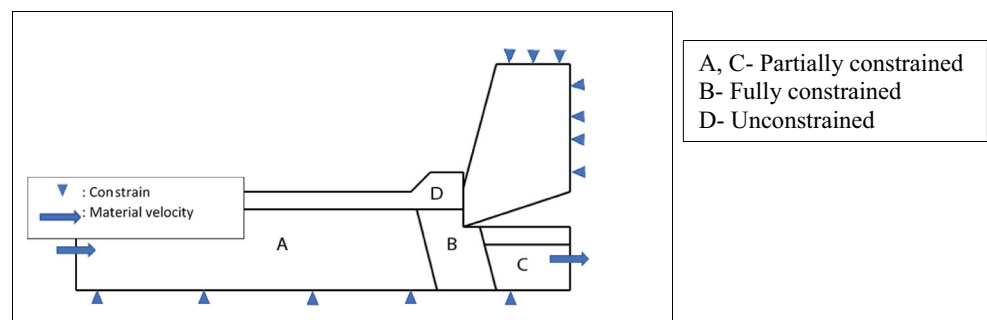




**Table 7** Johnson-Cook material parameters for AISI 4140 [23]

$A$ (MPa)	$B$ (MPa)	$C$	$n$	$m$
612 MPa	436 MPa	0.0134	0.15	1.46

50 m. At the same length of cut, the temperature rise is around 38% for all the prepared edges. This result can be attributed to the geometrical changes of the cutting tool as the tool wears out. The unprepared cutting tool has greater tool wear than prepared cutting tools. The higher tool wear produces a large flank area which eventually creates more abrasion of the tool with the workpiece surface, increasing the temperature on the flank face. It is reported in literature that the temperature increases as the tool wears out in all the cutting tools [34].

Initially, the unprepared cutting tool had a smaller edge radius of  $3\ \mu\text{m}$  and the stress was concentrated near the tool tip, resulting in a higher value of von Mises (VM) stress, Fig. 17. However, the maximum VM stress is reduced by 18.5% in all the prepared cutting tools. The maximum VM stress increases along with the cutting length in all the cutting edges. This behavior might be attributed to the larger flank area, which requires a greater amount of energy to deform the workpiece material. Therefore, the VM stress increases as the tool wears out [27]. Figure 17 shows that the worn unprepared tool has effective stress of 3900 MPa at a cutting length of 50 m. At the same stage, the maximum effective stress was around 3300 MPa in all the prepared cutting tools. The cutting edge prepared by drag finishing has lower stress than other prepared tools, but the difference is negligible.

Figure 18 shows the spatial distribution of temperature and von Mises stress on the tool with initial edge for the reference unprepared case and the three other prepared cases. It can be observed in Fig. 18a–d that, although the maximum temperature is close (717 to 739 °C), the general profile of temperature is affected by the edge preparation. Since the temperature

distribution depends on the heat generation due to plastic deformation in different regions and friction condition at the interface, two major regions are close to tooltip and away on the rake face where sliding friction occurs. A larger edge radius due to edge preparation increases the contact area with the workpiece, which eventually creates more deformation and higher cutting forces [8]. It results in higher temperature on the tool surface as well as more in-depth temperature distribution for the three prepared edges, Fig. 18b–d. Figure 18 e–h shows that the VM stress for the unprepared edge is much higher at the tooltip as compared to all prepared edges due to smaller edge radius. Since the tool is modeled as elastic material, stress values are high and the effective stress on the cutting tool indicates the risk of plastic deformation and damage to it [35].

The spatial temperature distribution of the worn tool at a cutting length of 50 m for all edges is shown in Fig. 19a–d. It can be observed that the maximum temperature is localized on the flank face of the unprepared edge. In the prepared edges, the high temperature is distributed on both the rake and flank faces. It has been reported earlier that after a certain edge radius limit, the maximum von Mises stress shifts from the rake face to the flank face continuing to increase along with increments of edge radius due to wear [36]. Similar behavior was observed in the current numerical study while investigating the stress behavior at different cutting lengths as shown in Fig. 19e–h.

### 3 Conclusions

This paper investigated the influence of three different cutting-edge preparation techniques (wet abrasive jet machining (WAJM), brushing, and drag finishing) on tool surface characteristics, tool performance, cutting forces and machined surface finish during orthogonal machining of AISI 4140 alloy steel. The major contributions and results of this study are listed below:

**Fig. 15** Methodology of updating the worn tool geometry. **a** Finding flank face. **b** Drawing displacement vector. **c** Worn tool

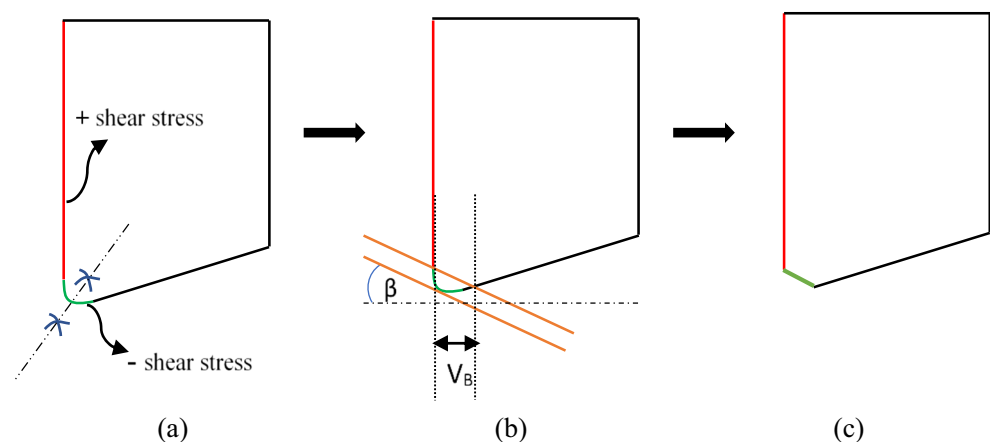
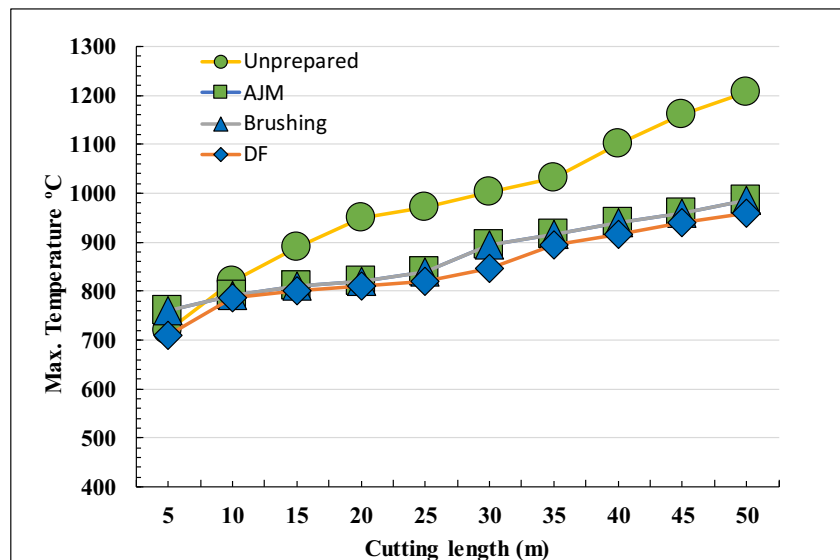


**Fig. 16** Variation in maximum temperature on the flank face



1. The cutting edge prepared by drag finishing demonstrated better performance than other preparation methods in terms of edge surface quality, lowest cutting forces, longest tool life, minimal flank wear, and the least roughness on the machined surface.
2. The compressive residual stress and edge hardness of the prepared edges are higher than that of the unprepared edge, where a 62.7% greater compressive stress is induced by abrasive jet machining.
3. Cutting edge prepared by AJM is about 91% rougher (in terms of  $Ra$ ) than the unprepared edge. In contrast, roughness is reduced by about 22% and 38.6% in edges prepared by brushing and drag finishing, respectively.
4. Tool flank wear in the prepared edges gradually grows, whereas flank wear in the unprepared edge increases dramatically after around 30 m. Edge preparation techniques helped reduce catastrophic wear, which is beneficial for planning machining operations.
5. The thermomechanical behavior predicted by finite element analysis shows an increase in both maximum temperature and von Mises stress in all the studied tools. However, the magnitude and rate of change are less in the prepared edges than in the unprepared edge. In addition, the distribution is also more spread out in the prepared edges, which reduces the magnitudes.

**Fig. 17** Variation in VM stress on the flank face

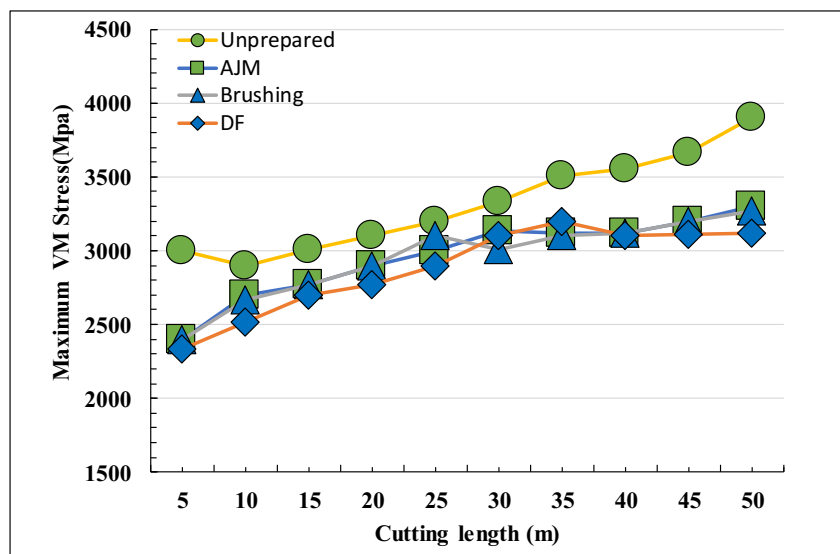
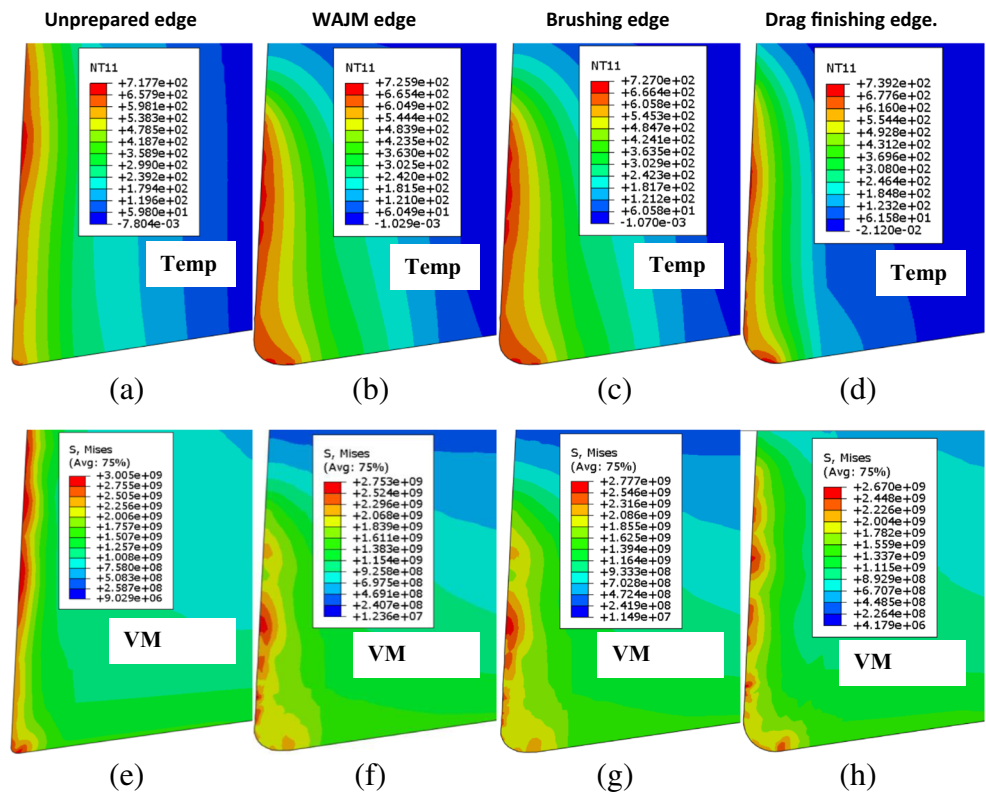


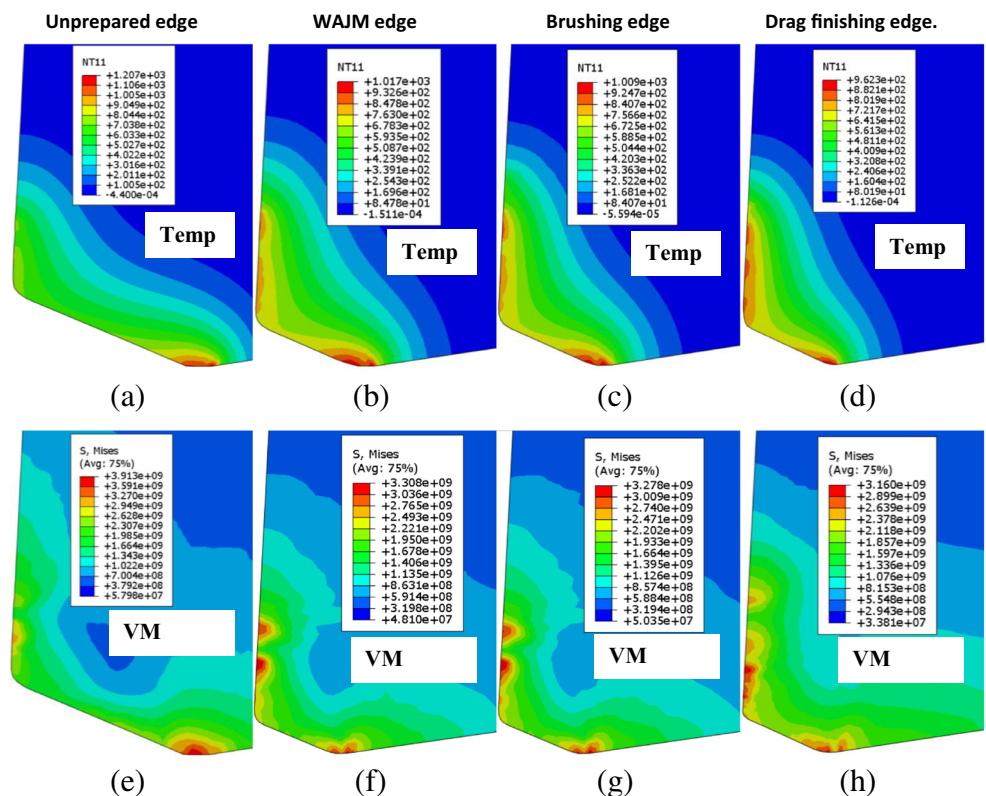
Fig. 18 Spatial distribution of temperature (a–d) and von Mises stress (e, f) for initial edge



6. The simulation predictions are consistent with experimental results. The high values of temperature and stress explain the

high tool wear rate in the unprepared cutting tool. The drag-finished edge was found to have the lowest flank wear rate.

Fig. 19 Spatial distribution of temperature (a–d) and von Mises stress (e, f) on worn tool at cutting length = 50 m



**Acknowledgments** The authors are thankful to BERKS Machine Tools, Ontario, Canada, for preparing brushing and drag finishing samples and Institute of Machining Technology, Technische Universität Dortmund, Germany, for preparing wet abrasive jet machining samples.

**Funding information** This research was supported by Natural Sciences and Engineering Research Council of Canada (NSERC) under the CANRIMT Strategic Research Network Grant NETGP 479639-15.

## References

- Rodríguez C (2009) Cutting edge preparation of precision cutting tools by applying micro-abrasive jet machining and brushing. Kassel university press GmbH, Kassel
- Byrne G, Dornfeld D, Denkena B (2003) Advancing cutting technology. *CIRP Ann Manuf Technol* 52(2):483–507
- Denkena B, Biermann D (2014) Cutting edge geometries. *CIRP Ann Manuf Technol* 63(2):631–653
- Denkena B, Köhler J, Ventura CEH (2013) Customized cutting edge preparation by means of grinding. *Precis Eng* 37(3):590–598
- Denkena B, Köhler J, Breidenstein B, Abrão AM, Ventura CEH (2014) Influence of the cutting edge preparation method on characteristics and performance of PVD coated carbide inserts in hard turning. *Surf Coat Technol* 254:447–454
- Wyen C-F (2011) Rounded cutting edges and their influence in machining titanium. ETH, Zürich
- Biermann D, Aßmuth R, Schumann S, Rieger M, Kuhlenkötter B (2016) Wet abrasive jet machining to prepare and design the cutting edge micro shape. *Procedia CIRP* 45:195–198
- Wyen C-F, Wegener K (2010) Influence of cutting edge radius on cutting forces in machining titanium. *CIRP Ann Manuf Technol* 59(1):93–96
- Krebs E, Wolf M, Biermann D, Tillmann W, Stangier D (2018) High-quality cutting edge preparation of micromilling tools using wet abrasive jet machining process. *Prod Eng* 12(1):45–51
- Bouzakis KD, Michailidis N, Skordaris G, Kombogiannis S, Hadjiyiannis S, Efstathiou K, Erkens G, Rambadt S, Wirth I (2002) Effect of the cutting edge radius and its manufacturing procedure, on the milling performance of PVD coated cemented carbide inserts. *CIRP Ann Manuf Technol* 51(1):61–64
- Denkena B, Bassett E, Köhler J (2012) On the honed cutting edge and its side effects during orthogonal turning operations of AISI1045 with coated WC-Co inserts. *CIRP J Manuf Sci Technol* 5:108–126
- Wang H, Yu A, Dong L, Wu L (2011) Edge preparation of carbide tools with abrasive brushing method. 2011 2nd Int. Conf. Mech. Autom. Control Eng. MACE 2011 - Proc., pp 256–259
- Fulemova J, Janda Z (2014) Influence of the cutting edge radius and the cutting edge preparation on tool life and cutting forces at inserts with wiper geometry. *Procedia Eng* 69:565–573
- Uhlmann E, Oberschmidt D, Löwenstein A, Kuche Y (2016) Influence of cutting edge preparation on the performance of micro milling tools. *Procedia CIRP* 46:214–217
- Yussefia NZ (2012) Cutting edge microgeometry modeling & electro-erosion honing. McMaster University
- Wang W, Biermann D, Aßmuth R, Arif AFM, Veldhuis SC (2020) Effects on tool performance of cutting edge prepared by pressurized air wet abrasive jet machining (PAWAJM). *J Mater Process Technol* 277(May 2019):116456
- Shia C-Y, Stango RJ, Heinrich SM (1998) Analysis of contact mechanics for a circular filamentary brush/workpart system. *J Manuf Sci Eng* 120(4):715
- Bouzakis KD, Michailidis N, Skordaris G, Kombogiannis S, Hadjiyiannis S, Efstathiou K, Pavlidou E, Erkens G, Rambadt S, Wirth I (2003) Optimisation of the cutting edge roundness and its manufacturing procedures of cemented carbide inserts, to improve their milling performance after a PVD coating deposition. *Surf Coat Technol* 163–164:625–630
- Yen Y-C, Jain A, Altan T (Feb. 2004) A finite element analysis of orthogonal machining using different tool edge geometries. *J Mater Process Technol* 146(1):72–81
- Özel T, Zeren E (2007) Finite element modeling the influence of edge roundness on the stress and temperature fields induced by high-speed machining. *Int J Adv Manuf Technol* 35(3–4):255–267
- AZoM, AZO MATERIALS, AISI 4140 Alloy Steel (UNS G41400), [AZoM.com - An AZoNetwork Site](https://www.azom.com/article.aspx?ArticleID=6769), 2012. [Online]. Available: <https://www.azom.com/article.aspx?ArticleID=6769>. [Accessed: 01-Dec-2018]
- Ma J, Ge X, Chang SI, Lei S (2014) Assessment of cutting energy consumption and energy efficiency in machining of 4140 steel. *Int J Adv Manuf Technol* 74(9–12):1701–1708
- Lee T (2007) An experimental and Theoretical investigation for the machining of hardened alloy steels. The University of New South Wales
- Maňková I, Vrabel M, Durakbasa NM (2016) Evaluation of cutting edge microgeometry for uncoated and coated end milling cutter. In: *Proceedings of 8th International Engineering Symposium*, p 54
- Thiele JD, Melkote SN (1999) Effect of cutting edge geometry and workpiece hardness on surface generation in the finish hard turning of AISI 52100 steel. *J Mater Process Technol* 94(2):216–226
- Oraby SE, Hayhurst DR (2004) Tool life determination based on the measurement of wear and tool force ratio variation. *Int J Mach Tools Manuf* 44:1261–1269
- Hosseinkhani K, Ng E (2013) Analysis of the cutting mechanics under the influence of worn tool geometry. *Procedia CIRP* 8:117–122
- Nasr MNA, Ng EG, Elbestawi MA (2007) Modelling the effects of tool-edge radius on residual stresses when orthogonal cutting AISI 316L. *Int J Mach Tools Manuf* 47(2):401–411
- Nasr MNA, Ng EG, Elbestawi MA (2008) A modified time-efficient FE approach for predicting machining-induced residual stresses. *Finite Elem Anal Des* 44(4):149–161
- Claudin C, Rech J, Grzesik W, Zalisz S (2008) Characterization of the frictional properties of various coatings at the tool/chip/workpiece interfaces in dry machining of AISI 4140 steel. *Int J Mater Form* 1(SUPPL. 1):511–514
- Yen Y, Söhner J, Lilly B, Altan T (2004) Estimation of tool wear in orthogonal cutting using the finite element analysis. 146:82–91
- Binder M, Klocke F, Doebbeler B (2017) An advanced numerical approach on tool wear simulation for tool and process design in metal cutting. *Simul Model Pract Theory* 70:65–82
- K. Hosseinkhani and E. Ng, A hybrid experimental and simulation approach to evaluate the calibration of tool wear rate models in machining, 2018
- Wanigarathne PC, Kardekar AD, Dillon OW, Poulachon G, Jawahir IS (2005) Progressive tool-wear in machining with coated grooved tools and its correlation with cutting temperature. *Wear* 259(7–12):1215–1224
- Agmell M, Ahadi A, Gutnichenko O, Ståhl JE (2017) The influence of tool micro-geometry on stress distribution in turning operations of AISI 4140 by FE analysis. *Int J Adv Manuf Technol* 89(9–12):3109–3122
- Al-Zkeri I, Rech J, Altan T, Hamdi H, Valiorgue F (2009) Optimization of the cutting edge geometry of coated carbide tools in dry turning of steels using a finite element analysis. *Mach Sci Technol* 13(1):36–51

**Publisher's note** Springer Nature remains neutral with regard to jurisdictional claims in published maps and institutional affiliations.